# Systematic Mapping of the Hubbard Model to the Generalized t-J Model

Alexander Reischl, Erwin Müller-Hartmann, and Götz S. Uhrig Institut für Theoretische Physik, Universität zu Köln, Zülpicher Str. 77, D-50937 Köln, Germany (Dated: November 6, 2018)

The generalized t-J model conserving the number of double occupancies is constructed from the Hubbard model at and in the vicinity of half-filling at strong coupling. The construction is realized by a self-similar continuous unitary transformation. The flow equation is closed by a truncation scheme based on the spatial range of processes. We analyze the conditions under which the t-J model can be set up and we find that it can only be defined for sufficiently large interaction. There, the parameters of the effective model are determined.

PACS numbers: 71.10.Fd, 75.10.Jm, 71.27.+a, and 71.30.+h

## I. INTRODUCTION

The Hubbard model serves as a prototype model for the description of strongly correlated electron systems. It consists of electrons with spin moving on a lattice. They repel each other on-site which leads to a complex interplay of magnetic and charge degrees of freedom. At half-filling, the model displays insulating behavior in the limit of strong interaction. In this limit, the model can be mapped onto a pure spin Heisenberg  $model^{1,2,3,4,5,6}$ . On the other side, vanishing interaction makes it a metal. In-between an intricate metal-insulator transition (MIT) takes place which is well understood only in extreme cases. In one dimension, the Bethe ansatz tells us that arbitrarily small interactions render the model insulating<sup>7</sup>. In infinite dimensions, the dynamical mean-field theory allows to make statements about the value of the critical interaction<sup>8,9,10</sup> if long-range magnetic order is suppressed. It is argued that this suppression can be achieved physically by introducing frustration.

It is the aim of the present paper to provide a systematic and controlled non-perturbative derivation of the t-Jmodel from the Hubbard model. Most importantly, we will discuss under which circumstances the reduction of the Hubbard model to a t-J model is justified. The t-Jmodel is the effective model describing fermions which interact and hop without creating or annihilating double occupancies (DOs). This means that never two electrons occur on the same site. Thus the reduction to a t-J model corresponds to the elimination of charge fluctuations. The parameters of the effective model will be computed quantitatively. Our results reach in two ways beyond what has been done before<sup>1,2,3,4,5,6</sup>. First, we provide non-perturbative results. Second, we discuss the matrix elements of hole motion and interaction in a systematic way beyond the zeroth order. Both ingredients help us to discuss the breakdown of the reduction to a t-J model.

The reference ensemble in our approach is the magnetically completely disordered half-filled model (see Sect. III). This constitutes the vacuum in our calculations. In this sense, we start from the Hubbard model at half-filling. But our approach naturally keeps also track of the dynamics of holes. This is unavoidable since we have

to know how virtual intermediate states evolve and they contain generically charge excitations. The parts of the effective model which describe the dynamics of holes apply also to holes inserted externally by doping. In this sense, the effective model describes also the physics of a vicinity of half-filling. But it is beyond the scope of the present paper to discuss the doping dependence of the couplings of the effective model since this would correspond to a change of the reference ensemble.

In Fig. 1 a schematic phase diagram is shown which

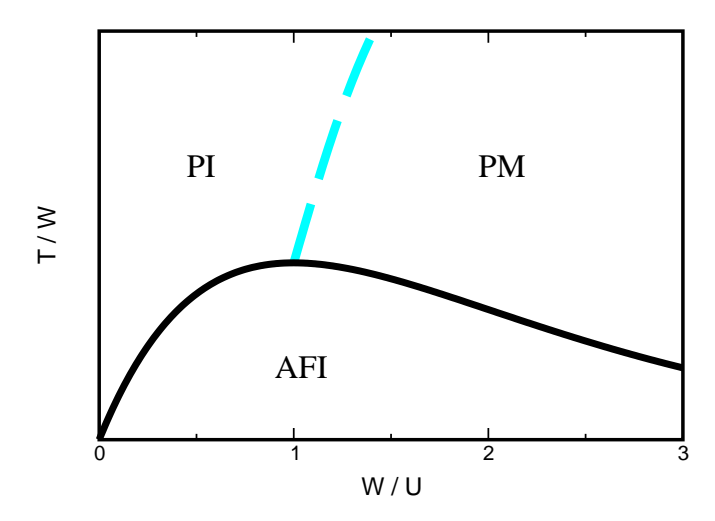


FIG. 1: Schematic phase diagram of the Hubbard model at half-filling in higher dimensions d>2. The tick labels at the x-axis are indicative only. The bare band width is denoted by W, the Hubbard repulsion by U, the temperature by T; PI stands for paramagnetic insulator, PM for paramagnetic metal and AFI for antiferromagnetic insulator. The dashed line indicates the transition or the crossover from insulator to metal.

summarizes the currently assumed picture. This picture is motivated from various mean-field computations, in particular in infinite dimensions<sup>9</sup>. For large repulsion U (left side in the figure), the electrons are localized so that the system is insulating. The spins interact via the magnetic exchange J of the order of  $4t^2/U$  which sets the energy scale for the transition between a long-range magnetically ordered phase (AFI) and a disordered phase

(PI). For decreasing U, the ground state remains insulating unless the magnetic order is fully suppressed. If the spin state becomes sufficiently disordered, for instance at higher temperatures, the system becomes conducting (PM). The change from paramagnetic insulator to paramagnetic metal is a first order transition in infinite dimensions and for not too large temperatures<sup>9</sup>. In general, it is to be expected that the system undergoes a crossover. In two dimensions in particular, the case investigated here, no long-range antiferromagnetism occurs at finite temperatures<sup>11</sup> so that the AFI collapses and only the disordered phases occur.

Once the interaction is such that the system is a paramagnetic metal, charge excitations are possible at zero energy. Hence, it cannot be expected that the elimination of charge fluctuations, virtual double occupancies, is possible. This means that the reduction of the Hubbard model to a t-J model can only be defined as long as the paramagnetic phase is insulating. The sole occurence of an insulating phase with long-range order is not sufficient. The insulating behavior in the long-range ordered AFI phase for interactions where the paramagnetic phase is metallic is due to the concomitant breaking of the translation symmetry. Hence it resembles rather a band insulator than a genuine Mott-Hubbard insulator<sup>12</sup>. The t-J model, however, describes low-lying degrees of freedom, namely the degrees of freedom of the spins and of doped charge carriers, without the precondition of a certain long-range order. The derivation of the t-J model requires to eliminate the virtual charge fluctuations while leaving the state of the spins and of the doped charges unspecified. One may consider the unspecified low-lying degrees of freedom to be at infinite temperature in a completely disordered mixture. The phase diagram in Fig. 1 tells us that there must be a certain U of the order of the band width W below which the Hubbard model cannot be represented by a t-J model.

The method of continuous unitary transformations (CUTs) has been proposed by Wegner in the context of condensed matter physics<sup>13</sup>. Simultaneously, similar approaches were tested by Głazek and Wilson in high energy physics<sup>14,15</sup>. The proper choice of an infinitesimal generator brings the many-body problem under study into a more tractable form by decoupling different sectors of the Hamiltonian. In many cases it is possible to advance to an effective model that is tractable by some other means while retaining the complex physics of the original problem<sup>6,16,17,18,19,20</sup>. We will apply a CUT to the Hubbard model in order to eliminate operators that couple states of different double occupancy. This has been done before by Stein<sup>6</sup> in a perturbative fashion. In contrast to Stein's perturbative treatment we will adopt a self-similar truncation scheme for the operators emerging during the transformation. This self-similar CUT retains terms of a certain structure.

The paper is organized as follows. The Hubbard model is introduced in Sect. II. Sect. III explains the method of self-similar CUTs. A transparent example is given to

illustrate technical details and characteristic properties of the CUT applied to the Hubbard model. The results for the range of validity of the mapping and for the effective parameters are presented in Sect. IV. Evidence is provided that the mapping cannot be defined for all ratios W/U. The physical implications of our findings are discussed in Sect. V. A brief summary is given finally in Sect. VI.

## II. HUBBARD MODEL AND OPERATORS

Our starting point is the Hubbard model on a twodimensional square lattice in the vicinity of half-filling with nearest-neighbor hopping. Since the calculation covers also the motion and interaction of charge carriers it is not limited to strictly half-filling but covers also small hole concentrations.

The Hamilton operator is split into a kinetic part  $H_t$  and an interaction  $H_U$ 

$$H = H_U + H_t \tag{1a}$$

$$H_U = U \sum_{i} (n_{i,\uparrow} - 1/2)(n_{i,\downarrow} - 1/2)$$
 (1b)

$$= (U/2) \left( \hat{D} - N/2 \right)$$

$$H_t = t \sum_{\langle i,j \rangle, \sigma} (c_{i,\sigma}^{\dagger} c_{j,\sigma} + \text{h.c.}), \qquad (1c)$$

where N is the number of sites,  $c_{i,\sigma}^{\dagger}$ ,  $c_{i,\sigma}$  are creation and annihilation operators of an electron on site i with spin  $\sigma \in \{\uparrow,\downarrow\}$  and  $n_{i,\sigma} = c_{i,\sigma}^{\dagger} c_{i,\sigma}$  is the number operator. Hopping is only possible between nearest neighbor (NN) sites as indicated by  $\langle i,j\rangle$  in the sum in  $H_t$ . The bare hopping coefficient is given by t so that in two dimensions the band width is W = 8t. It turns out to be convenient to denote all results in terms of the band width W.

We also define the operator  $\hat{D} := \sum_{i} [n_{i,\uparrow} n_{i,\downarrow} + (1 - n_{i,\uparrow})(1 - n_{i,\downarrow})]$  that counts the number of double occupancies (DOs) of particles and holes.  $H_U$  describes the repulsion of electrons of opposite spin on the same site. For large U the density of states splits into an upper and a lower Hubbard band separated by an energy of order U. In the half-filled case, in the limit of infinite U the electrons are fixed on their lattice site by the constraint of having no DO. Reducing U from this limit the electrons are gradually allowed to move producing DOs intermediately. But the physics remains still rather local. In the following, we want to map the Hubbard model for finite U in a systematic way onto an effective model that conserves the number of DOs. The guiding idea will be that the physics can be incorporated into an effective model that contains operators that describe rather local processes. For too small values of U the vanishing of the charge gap will make the mapping impossible.

# III. CONTINUOUS UNITARY TRANSFORMATION

In this section, the technical details of our calculations are presented. The method of continuous unitary transformations (CUT) introduces a continuous auxiliary variable  $\ell$  and transforms the Hamiltonian according to the flow equation  $^{13}$ 

$$\frac{d}{d\ell}H(\ell) = [\eta(\ell), H(\ell)] \tag{2}$$

with an antihermitian generator  $\eta(\ell)$ . The operators  $H(\ell)$  for different values of  $\ell$  are unitarily equivalent. The transformation starts with the initial condition  $H(\ell=0)=H$  and ends with an effective Hamiltonian at  $\ell\to\infty$ . We want the effective Hamiltonian to conserve the number of DOs and therefore use the generator<sup>6</sup>

$$\eta(\ell) = [\hat{D}, H(\ell)] . \tag{3}$$

Except for an overall factor<sup>21</sup>, the above  $\eta$  coincides with  $\eta$  in Refs. 17,22, where it was defined using the sign of the change in the number of quasiparticles ensuring that the block-band structure of the Hamiltonian is conserved. This means that during the flow no operators are generated that change the number of DOs by a value other than 0, -2 and 2.

To see how the CUT works, it is helpful to classify the operators in the kinetic part of the hamiltonian according to their effect on the number of DOs

$$H_{t} = T_{0} + T_{+2} + T_{-2}$$

$$T_{0} = t_{0} \sum_{\langle i,j \rangle, \sigma} \left[ (1 - n_{i,\sigma}) c_{i,\overline{\sigma}}^{\dagger} c_{j,\overline{\sigma}} (1 - n_{j,\sigma}) + n_{i,\sigma} c_{i,\overline{\sigma}}^{\dagger} c_{j,\overline{\sigma}} n_{i,\sigma} + \text{h.c.} \right]$$

$$(4a)$$

$$\begin{split} T_{+2} &= t_{+2} \sum_{\langle i,j \rangle,\sigma} \left[ n_{i,\sigma} c_{i,\overline{\sigma}}^{\dagger} c_{j,\overline{\sigma}} (1 - n_{j,\sigma}) \right. \\ &\left. + n_{j,\sigma} c_{j,\overline{\sigma}}^{\dagger} c_{i,\overline{\sigma}} (1 - n_{i,\sigma}) \right] \end{split} \tag{4c}$$

$$\begin{split} T_{-2} \; = \; t_{-2} \sum_{\langle i,j \rangle,\sigma} \left[ (1-n_{i,\sigma}) c_{i,\overline{\sigma}}^{\dagger} c_{j,\overline{\sigma}} n_{j,\sigma} \right. \\ & + (1-n_{j,\sigma}) c_{j,\overline{\sigma}}^{\dagger} c_{i,\overline{\sigma}} n_{i,\sigma} \right] \,, \ \, (\text{4d}) \end{split}$$

where  $\overline{\sigma} = -\sigma$ . The projection operators ensure that  $T_n$  changes the number of DOs by n.

Operators will be denoted in a standardized normalordered real space representation (see Table I). The prefactors of such a product of local operators will be called *coefficient* of this term in the Hamiltonian. Eq. (2) will yield differential equations for these coefficients. The coefficients  $t_0$ ,  $t_{+2}$  and  $t_{-2}$  coincide and are equal to the bare hopping t in the beginning of the transformation. But they will develop differently during the flow. The operator  $T_n$  yields a contribution  $[\hat{D}, T_n(\ell)] = nT_n(\ell)$  to  $\eta$  leading to

$$\frac{d}{d\ell}H = [\eta, H_U] + \dots = -\frac{U}{2}n^2T_n(\ell) + \dots$$
 (5)

and thus to a suppression of any term not conserving the number of DOs.

In general the prescription (2) will not produce closed equations. One has to find a way to deal with the proliferating number of terms. Stein<sup>6</sup> set up a perturbative CUT for the Hubbard model with the same generator (3). He ordered the terms produced on the right hand side of (2) according to the power of t/U with which they were generated. The terms were kept in a form consisting of long products of  $T_0$ ,  $T_{+2}$  and  $T_{-2}$ .

Contrary to this perturbative strategy, we will not keep the commutators of  $T_0$ ,  $T_{+2}$  and  $T_{-2}$  in the unevaluated form. We compute the right hand side of the flow equation (2) explicitly. This will produce terms already present in the Hamiltonian and new terms. According to systematic rules the new terms will be kept or discarded. Finally, a closed set of terms is reached. The differential equations representing the flow equations of the CUT are obtained by comparing the coefficients of all the retained terms. Since both  $\eta$  and H are linear in the coefficients the right hand sides of the differential equations are bilinear in the coefficients in close analogy to conventional renormalization group equations.

To find a scheme to truncate the generation of new terms we make the following considerations. In the limit of large U the motion of the electrons at half-filling is suppressed by the energy cost of DOs. Therefore the operators that become important first when going to lower U are those that describe local processes. To use this for the truncation scheme we have to define a measure for the locality of a term. An undispensable prerequisite is a physically meaningful and in particular unique way to denote the operators. Hence we define a sort of normal-ordering of the operator products<sup>23</sup>. We will normal-order all terms with respect to the half-filled paramagnetic reference ensemble represented by the statistical operator

$$\hat{\rho}_0 := \prod_i (1/2)(|\uparrow\rangle_{ii}\langle\uparrow| + |\downarrow\rangle_{ii}\langle\downarrow|) \tag{6}$$

where we use a basis of local states at each site i. There are four local states: the empty site  $|0\rangle$ , two singly occupied states with spin up und down,  $|\uparrow\rangle$  and  $|\downarrow\rangle$ , and the state with two electrons,  $|\uparrow\downarrow\rangle$ . The reference ensemble (6) contains only states with one electron per site since it is half-filled. The up-spin and down-spin states are weighted equally to represent a completely disordered paramagnetic reference ensemble. Any deviation from the reference ensemble represents an excitation.

A product of n local operators  $\mathcal{O}_1 \cdot ... \cdot \mathcal{O}_n$  is normal-ordered if any expectation value

$$\langle \mathcal{O}_i \rangle_{\text{ref}} := \text{Tr}(\mathcal{O}_i \hat{\rho}_0)$$
 (7a)

$$= (1/2)({}_{i}\langle\uparrow|\mathcal{O}_{i}|\uparrow\rangle_{i} + {}_{i}\langle\downarrow|\mathcal{O}_{i}|\downarrow\rangle_{i})$$
 (7b)

with the reference ensemble vanishes. In Table I all local operators are given in their normal-ordered form. Apart from the unity matrix 1 all local operators in Tab. I are chosen such that the expectation value (7) with the reference ensemble yields zero. The operator  $\bar{n}=n_{\uparrow}+n_{\downarrow}-1$  counts the number of electrons relative to half-filling. The Hubbard operator  $2n_{\uparrow}n_{\downarrow}-\bar{n}$  counts the number of DOs. The empty state  $|0\rangle$  and the doubly occupied state  $|\uparrow\downarrow\rangle$  yield  $\langle 0|2n_{\uparrow}n_{\downarrow}-\bar{n}|0\rangle=\langle\uparrow\downarrow|2n_{\uparrow}n_{\downarrow}-\bar{n}|\uparrow\downarrow\rangle=1$  whereas expectation values with  $|\uparrow\rangle$  and  $|\downarrow\rangle$  vanish. For the spin operator  $\sigma^z$  the sum (7) is zero as well. All other operators in Table I are non-diagonal in the local basis and thus normal-ordered with respect to the reference ensemble.

$$\begin{array}{|c|c|c|c|c|}\hline & & & & \\ \hline \sigma^z = n_\uparrow - n_\downarrow \\ (1-n_\downarrow)c_\uparrow \\ (1-n_\downarrow)c_\uparrow^\dagger \\ \hline \end{array} \begin{array}{|c|c|c|c|c|c|c|}\hline n = n_\uparrow + n_\downarrow - 1 & \sigma^+ = c_\uparrow^\dagger c_\downarrow & c_\downarrow c_\uparrow \\ 2n_\uparrow n_\downarrow - \bar{n} & \sigma^- = c_\downarrow^\dagger c_\uparrow & c_\uparrow^\dagger c_\downarrow^\dagger \\ (1-n_\uparrow)c_\downarrow & n_\uparrow c_\downarrow & n_\uparrow c_\uparrow^\dagger \\ (1-n_\uparrow)c_\downarrow^\dagger & n_\uparrow c_\uparrow^\dagger & n_\downarrow c_\uparrow^\dagger \\ \hline \end{array}$$

TABLE I: Local operators. The operators in the first two lines have an even number of fermionic operators, those in the last two lines an odd number of fermionic operators; the usual spin operators are  $S^z = \sigma^z/2$ ,  $S^{\pm} = \sigma^{\pm}$ .

The local operators of Tab. I have to be labelled with a site-index when they are used to write down the Hamiltonian. Consequently, also products of local normal-ordered operators belonging to different sites are normal-ordered. The expectation values of each separate factor with respect to the reference ensemble vanish. It is the prefactor of a product of local operators as defined in Tab. I which we will call the *coefficient* of this term.

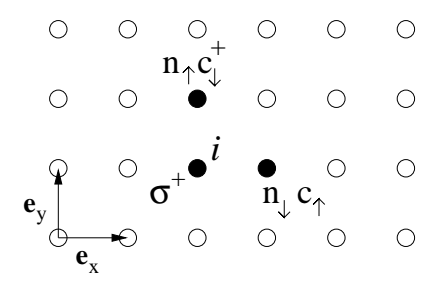


FIG. 2: The operator from Eq. 8 in the 2-dimensional square lattice. Filled sites are involved in the hopping process. The operators are shown at the sites on which they act.

On the basis of the normal-ordering and of the standardized notation introduced above we define a measure for the locality of a term, namely its extension d. Consider the following exemplary normal-ordered term

$$\sum_{i} n_{i+\mathbf{e}_{y},\uparrow} c_{i+\mathbf{e}_{y},\downarrow}^{\dagger} c_{i+\mathbf{e}_{x},\uparrow} n_{i+\mathbf{e}_{x},\downarrow} \cdot \sigma_{i}^{+}. \tag{8}$$

This term represents the hopping of an electron from site  $i + \mathbf{e}_x$  to site  $i + \mathbf{e}_y$ . The spin of the electron is flipped in

this process, which is compensated by the spin-flip on site i. This term is illustrated in Fig. 2. It contains operators that act on three different sites. They are shown as filled circles in Fig. 2. These sites will be called the *cluster* belonging to this term. The maximal taxi cab distance d of two sites in this cluster is the *extension* of this term. The extension of the term (8) in Fig. 2 is d=2. The extension of the cluster belonging to a term will be our measure of its locality. For a truncation scheme, we define a certain set of clusters, i.e. geometric arrangements of sites which are translated over the whole lattice. Those operators generated in the flow equation (2) are kept which can be defined completely on one of the clusters. If they affect more sites or sites at a larger distance the operators are discarded.

We emphasize that the use of a set of clusters to define the truncation does not turn our approach into a finite cluster calculation. Rather it is a self-similar, renormalizing calculation in the thermodynamic limit where the decision which terms are kept is based on their locality. By translational invariance, the operators appear in the whole lattice as is denoted by the  $\sum_i$  in Eq. (8). For large enough clusters, the perturbative results are reproduced by the self-similar calculation. For simplicity, the differential equation is set up for the coefficient of a single representative of a certain kind of term taking advantage of the symmetries of the problem, namely translational invariance, the point-group symmetries, spin rotation symmetry, and hermiticity.

The complete prescription for the self similar CUT calculation reads: (i) Define a certain set of clusters. Normal-ordered operators on these clusters are kept during the calculation. Additional conditions may be imposed. With this truncation rule the flow equation (2) closes. (ii) Calculate  $[\eta(\ell), H(\ell)]$  to obtain the flow equation (2) for the coefficients of the terms in H. Terms not present in the original Hamiltonian start at  $\ell=0$ with initial coefficients zero. (iii) The numerical integration of the flow equation yields the effective model for  $\ell \to \infty$ ; it conserves the number of DOs. This step requires that the flow equation converges for  $\ell \to \infty$ . If it converges the effective model is constructed successfully. Generally, non-convergence can be due to an insufficient approximation or due to the breakdown of the mapping of the Hubbard model to the t-J model.

Our procedure for a self similar CUT calculation will be exemplified in the following subsection.

# A. Example: The minimal and the NN truncation

Here we work out a simple example and compare its results to perturbation theory. At first we build a minimal model for the NN coupling J. Starting with  $H_t$  and  $H_U$  the generator  $\eta$  reads

$$\eta(\ell) = [\hat{D}, H(\ell)] = [\hat{D}, T_{+2} + T_{-2}] = 2T_{+2} - 2T_{-2}$$
 (9)

To set up the flow equation we have to calculate

$$\frac{d}{d\ell}H(\ell) = [\eta(\ell), H(\ell)] = [\eta(\ell), H_U(\ell) + H_t(\ell)]. \quad (10)$$

The first contribution to the flow equation

$$[\eta(\ell), H_U(\ell)] = -2U(\ell)T_{+2} - 2U(\ell)T_{-2} \tag{11}$$

produces the suppression of terms changing the number of DOs as intended. The second contribution reads

$$[\eta(\ell), H_t(\ell)] = [2T_{+2} - 2T_{-2}, T_0 + T_{+2} + T_{-2}]$$
  
=  $32t_{+2}t_{-2} \cdot \frac{1}{2}\hat{D}$  (12a)

$$+16t_{+2}t_{-2}\sum_{\langle i,j\rangle}\mathbf{S}_i\cdot\mathbf{S}_j\tag{12b}$$

$$-4t_{+2}t_{-2}\sum_{\langle i,j\rangle}\bar{n}_i\bar{n}_j \tag{12c}$$

$$+8t_{+2}t_{-2}\sum_{\langle i,j\rangle}c_{i,\uparrow}^{\dagger}c_{i,\downarrow}^{\dagger}c_{j,\downarrow}c_{j,\uparrow}$$
 (12d)

+... (three site terms).

In Eq. (12) the terms containing operators on three different sites are omitted. The term (12a) will renormalize the strength of the Hubbard interaction U. The next line (12b) generates the Heisenberg exchange

$$H_{\rm NN} = J_1(\ell) \sum_{\langle i,j \rangle} \mathbf{S}_i \cdot \mathbf{S}_j \tag{13}$$

with the initial condition  $J_1(0)=0$ . To get a minimal model for the NN exchange we neglect the terms in (12c) and (12d). The exchange term  $H_{\rm NN}$  will not produce a contribution to  $\eta$  since it does not change the number of DOs. As a further simplification we neglect the terms that would arise from the commutator  $[\eta, H_{\rm NN}]$ . Exploiting that operators related by hermitian conjugation have the same coefficient we know  $t_{+2}=t_{-2}$ . Thus the differential equations for the minimal truncation read

$$d_{\ell}U(\ell) = 32t_{+2}(\ell)^2 \tag{14a}$$

$$d_{\ell}t_0(\ell) = 0 \tag{14b}$$

$$d_{\ell}t_{+2}(\ell) = -2U(\ell)t_{+2}(\ell) \tag{14c}$$

$$d_{\ell}J_{1}(\ell) = 16t_{+2}(\ell)^{2} , \qquad (14d)$$

where we use  $d_{\ell}$  as shorthand for  $\frac{d}{d\ell}$ . Using the conserved quantity  $s = \sqrt{64t_{+2}(\ell)^2 + 4U(\ell)^2}$  we obtain for the minimal truncation

$$U(\ell) = \frac{s}{2} \tanh(s\ell + C) \tag{15a}$$

$$t_0(\ell) = t_0(0) \tag{15b}$$

$$t_{+2}(\ell) = t_{-2}(\ell) = (s/8)\sqrt{1 - \tanh^2(s\ell + C)}$$
 (15c)

$$J_1(\ell) = s \left[ \tanh(s\ell + C) - 2U_0/s \right]/4$$
 (15d)

where  $C = \operatorname{arctanh}(2U_0/s)$ . The effective model is obtained in the limit  $\ell \to \infty$ . Since  $t_{+2}(\infty) = 0$  it contains only #DO-conserving terms

$$H_{\text{eff}} = T_0 + U(\infty) \frac{1}{2} \hat{D} + J_1(\infty) \sum_{\langle i,j \rangle} \mathbf{S}_i \cdot \mathbf{S}_j.$$
 (16)

Strictly at half-filling, Eq. (16) reduces to a Heisenberg model with effective coupling  $J_{1,\text{eff}} = J_1(\infty)$ 

$$J_{1,\text{eff}} = \frac{U}{2} \sqrt{1 + 16 (t/U)^2} - \frac{U}{2}$$
 (17a)  
=  $\frac{4t^2}{U} + \mathcal{O}(t^4/U^3)$ . (17b)

For small t/U this reproduces the well-known second order result<sup>4</sup>  $J_1^{(2)} = \frac{4t^2}{U}$ . Note that the final results are given in t and U denoting the initial, bare values whereas, for clarity, we use  $t_0 = t$  and  $U_0 = U$  to denote the initial, bare values while solving the flow equation.

FIG. 3: Filled circles indicate the two clusters defining the truncation rule of the NN truncation. Only terms fitting on these clusters are kept.

The result (17) coincides with the result one gets from diagonalization of a two-site cluster for the splitting between the singlet and the triplet state and thus for J. This is purely coincidental since taking into account *all* operators on NN sites in the CUT leads to a different result. The truncation rule for this NN truncation is defined by the two clusters shown in Fig. 3. All terms are kept that contain only local operators on two neighboring sites. For the effective coupling we find, see Appendix A,

$$J_{1,\text{eff}}^{\text{NN}} = \frac{2}{7}U\sqrt{1+28(t/U)^2} - \frac{2}{7}U$$
 (18)

As expected the result is different from the result for two sites since the exact diagonalization deals with a finite system only whereas the CUT is a renormalization procedure on the thermodynamic lattice where the terms kept are chosen according to their locality.

To compare our results to perturbation theory, we calculated also the 4th and 6th order in t/U for  $J_1$  in perturbation theory<sup>3,24</sup>. Fig. 4 compares the value of the Heisenberg coupling  $J_1$  from the minimal and from the NN truncation to the results from perturbation theory. All results are given relative to the second order result  $J_1^{(2)} = 4t^2/U$ . The perturbative results show strong divergencies even if one includes the 4th and the 6th order.

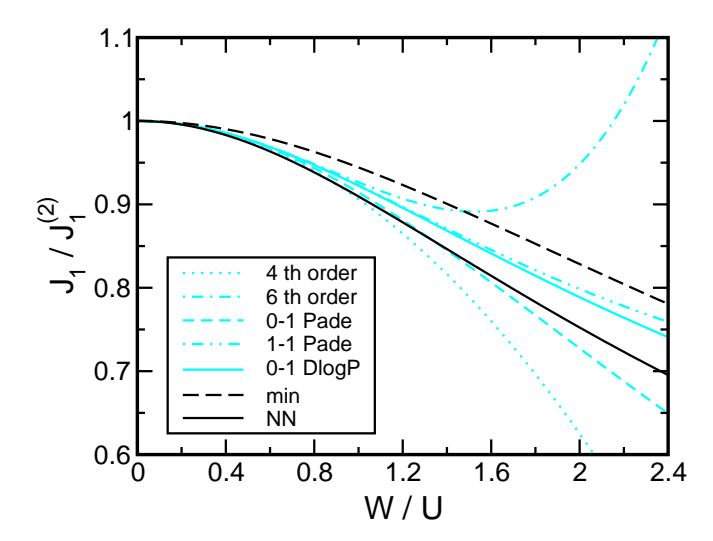


FIG. 4: Results for the Heisenberg coupling  $J_1$  from the minimal and the NN truncation compared to perturbation theory. All curves are plotted relative to  $J_1^{(2)} = 4t^2/U$ . The numbers in the legend in front of Padé or DlogP indicate the degree of the polynomials in  $x = t^2/U^2$  in the numerator and denominator of the Padé approximant. Recall W = 8t.

The dashed and solid black lines show the solution for  $J_1$  from the minimal and NN truncation, respectively. They give meaningful finite values for  $J_1$  without divergent behavior up to high values of W/U. Already the minimal model correctly reproduces the leading perturbative behavior  $\propto 4t^2/U$  for small W/U.

In addition, Fig. 4 shows Padé-approximants derived from the series of the perturbation theory. The continuous grey line depicts a Dlog-Padé-approximant. The Padé-approximants support that the CUT results for  $J_1$  lie in the reasonable range of values. But neither the CUT nor the Padé results determine  $J_1$  reliably for values of  $W/U \gtrsim 0.8$ . Therefore, we improve the CUT calculation by taking into account more terms on more complex site configurations leading to higher truncation schemes. The agreement of calculations with various numbers of operators will be a probe for the accuracy of the results.

# B. Higher truncation schemes

Fig. 5 shows the clusters defining the various truncation schemes. The sites that belong to the clusters are depicted as filled circles within the two-dimensional square lattice. Only one representative is shown for different clusters that are related by the point-group symmetry of the square lattice. We use the clusters that are necessary for a perturbative derivation of the spin Hamiltonian from the Hubbard model as a guideline for the choice of the clusters defining the truncation. In second order the NN Heisenberg exchange is the only effective spin-coupling. For its perturbative derivation a cluster of two

neighboring sites is sufficient. Thus the NN truncation is defined by the cluster given in Fig. 5a. The cluster in Fig. 5a represents the two possible clusters of NN sites on the two-dimensional square lattice. In 4th order in the electron hopping t also further hopping processes contribute to the effective spin-couplings. The cluster of four sites on a plaquette of the square lattice and the linear clusters of three sites cover all relevant hopping processes in 4th order. They are depicted in Fig. 5b. The double plaquette and the linear chain of four sites depicted in Fig. 5c are representatives for the clusters necessary for accounting fully of the 6th order.

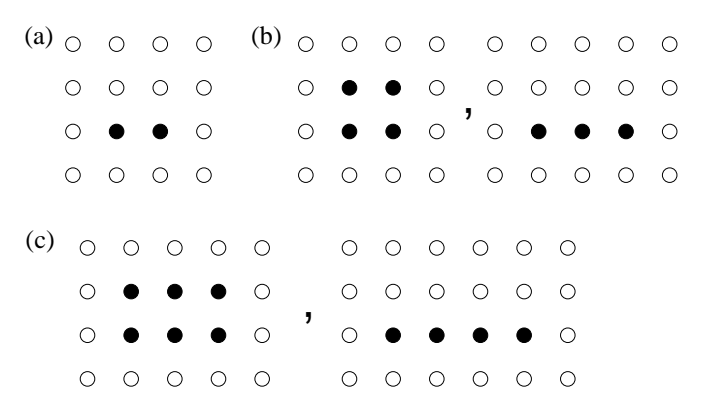


FIG. 5: Various clusters defining the operators to be kept in the CUT. Only one of various clusters that are related by the point group symmetry of the two-dimensional square lattice is shown.

The calculation for the clusters in Fig. 5c was the largest possible. To have an additional comparison, we also performed calculations keeping only the operators which affect at most four different sites on the clusters of Fig. 5c. In summary, the various truncation schemes are

- (i) **minimal** model: only  $H_U$ ,  $H_t$ ,  $H_{NN}$
- (ii) NN: cluster used in 2nd order perturbation theory, Fig. 5a.
- (iii) **plaquette** and three-site chain: cluster used in 4th order, Fig. 5b.
- (iv) operators on up to four different sites on the clusters of Fig. 5c.
- (v) **double-plaquette** and four site chain: clusters used in 6th order, see Fig. 5c.

The NN truncation (ii) yields the leading order result for the NN spin coupling  $J_1$ , the plaquette truncation (iii) yields the correct result in 4th order, and the double plaquette truncation (v) yields the correct result in 6th order. We confirmed that our implementation complies with these checks.

The computation of the effective model splits into two parts. First, one has to set up the flow equation, i.e., one has to calculate the commutator  $[\eta, H]$ . According

Calculation	# operators in ${\cal H}$	# of terms in DE
(i) minimal	4	3
(ii) NN	6	8
(iii) plaquette	172	10,364
(iv)	2,217	1,341,736
(v) double-plaquette	26,251	304,514,721

TABLE II: Number of operators in the Hamiltonian reduced by the symmetries given in the main text for various approximation schemes. This number coincides with the number of differential equations. In the last column the number of bilinear terms on the right hand side the differential equations is listed.

to the truncation scheme newly generated terms are discarded or included in H, in  $\eta$ , and in the calculation of  $[\eta,H]$ . This is done in a dynamic fashion in a C++ program. The list of terms considered grows in the course of the automatized computation of the commutators. Since we consider operators on a finite number of sites there is a point, when no new terms are generated. At this point the set of differential equations, the flow equation, is closed.

Second, one has to solve this flow equation. The differential equations have to be set up only once for each truncation scheme. Then they must be solved numerically for each set of initial conditions given by the initial value of t/U. Since all coefficients are entangled in the differential equations the numerical integration provides all the coefficients – magnetic exchange couplings, hopping and interactions of charge – of the effective model together.

To keep the number of terms as small as possible, we made use of the point-group symmetries of the square lattice, i.e., rotations about multiples of  $\pi/2$  and reflections about the axes and diagonals. Additionally, terms which are related by hermitian conjugation, by particlehole transformation, and by flipping  $\sigma \to -\sigma$  all spin indices carry the same coefficient. Table II shows the number of terms, reduced by the symmetries, in the Hamiltonian of each calculation. As  $\eta$  and H are both linear in the coefficients of the terms the right hand side of the differential equations is bilinear in these coefficients. The third column of Tab. II lists the number of such bilinear terms in the differential equation. The number of variables and the number of differential equations is growing fast with the size of the cluster defining the truncation rule. This renders both the set up of the flow equation and its numerical integration computationally costly.

We implemented the CUT calculation on the computer with two C++-programs. The first sets up the differential equation by symbolic calculation of the commutator of  $\eta$  and H. For a large number of terms in the hamiltonian this task is very time-consuming. But it is possible to split the calculation into a number of independent parts that can be accomplished by separate programs.

For the double plaquette, about 65 separate runs were performed, each with a CPU time below 10 hours and less than 0.5 Gbyte memory on Sun UltraSPARC workstations.

The second program solves the flow equation, i.e., the set of differential equations. As the set of equations is large this second program is very demanding both in time and in memory space. Typically 120 hours of CPU time and about 2.5 Gbyte are needed on Sun UltraSPARC workstations.

#### IV. RESULTS

Here we present the results for the five different truncation schemes (i) to (v) described above in Sect. III B. First, we discuss some properties of the continuous unitary transformation which enable us to analyze the limitations of the construction of the t-J model. Second, data on the effective magnetic couplings will be given. Third, data on the effective charge couplings will be shown.

# A. Properties of the CUT

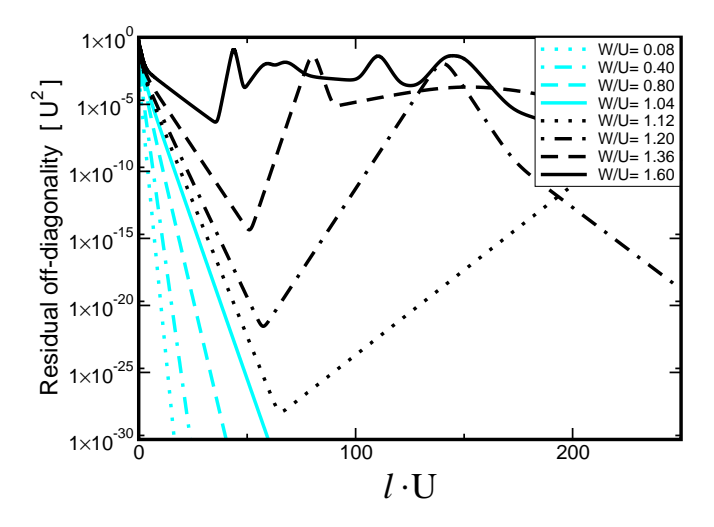


FIG. 6: Evolution of the residual off-diagonality in the double-plaquette calculation (v) for various values of W/U.

The CUT is induced by operators that change the number of DOs. They are off-diagonal in the number of DOs. We define the *residual off-diagonality* as the sum per site of the squares of all coefficients that belong to operators that change the number of DOs. In the calculation the Hamiltonian is written in terms of products of the local operators in Table I. This implies the definition of the coefficient as the prefactor of such a product.

The residual off-diagonality measures the extend to which the unitary transformation has eliminated the terms that change the number of DOs. In a numerical integration of the differential equation the residual off-diagonality will not vanish exactly. Therefore, we define a small but non-zero value and stop the flow when the residual off-diagonality falls below this value. Fig. 6 displays the evolution of the residual off-diagonality in the double-plaquette calculation (v) during the flow, parametrized by the variable  $\ell U$ , see Sect. III, for various values of W/U. At  $\ell=0$  the operators in  $T_{+2}$  and  $T_{-2}$  in (4) contribute to the residual off-diagonality. Written with the operators in Table I these are 4\*2=8 terms (hopping forth and back in x- and y-direction, with spin up or down) in  $T_{+2}$  and  $T_{-2}$  each. Therefore the curves in Fig. 6 for the residual off-diagonality start at  $\ell=0$  with the value  $8t_{+2}^2+8t_{-2}^2=16t^2$ .

For small values of W/U the residual off-diagonality shows exponential decay. For larger values of W/U the convergence is slower. For W/U=1.12 it shows for the first time pronounced non-monotonic behavior. The dotted black curve, corresponding to W/U=1.12, falls below  $10^{-27}$  to rise again up to  $10^{-3}$  for  $\ell \cdot U \approx 270$ . Non-monotonic behavior occurs for all values  $W/U \geq 1.12$ ; it can become a problem since we have to compare the residual off-diagonality to a small but finite value to decide at which value of  $\ell$  to stop the integration of the differential equations. But the values of the dominant coefficients of the effective model are reached already at small  $\ell$ . They are not affected noticeably by different cutoffs for the residual off-diagonality.

Most importantly, one has to check whether the mapping to the effective model is possible at all. Below we will calculate the apparent charge gap  $\Delta_{\rm app}$  within the effective model. This is the minimal energy of a DO, e.g. a hole, propagating through a paramagnetic spin background after the CUT. Since the paramagnetic spin background is not the ground state the apparent charge gap  $\Delta_{\rm app}$  is not the true charge gap. The apparent charge gap measures the separation of energy scales. This separation governs the convergence of the mapping as we perform it. We will discuss this issue and its physical significance in more detail in the Discussion.

We find that the apparent charge gap  $\Delta_{\rm app}$  becomes negative (!) for values of  $W/U\gtrsim 0.92$ . Once excitation energies become negative the CUT does not work because the limit  $\ell\to\infty$  does not exist any longer. The #DO-changing processes can no longer be eliminated because they constitute no longer vacuum fluctuations around a stable vacuum. The negativity of excitation energies signals that the chosen reference ceases to be a physically reasonable reference.

The non-monotonic behavior of the residual off-diagonality appears only in a parameter range where the mapping is no longer possible. For parameters  $W/U \lesssim 0.9$ , where the mapping is possible according to  $\Delta_{\rm app} > 0$ , we find an exponential decrease of the residual off-diagonality down to values where the calculation is limited by the numerical accuracy of the computer implementation. A pronounced increase of the residual off-diagonality was only found in the double-plaquette calculation (v). The calculations (i)–(iv) show an exponential

drop of the residual off-diagonality for all values W/U.

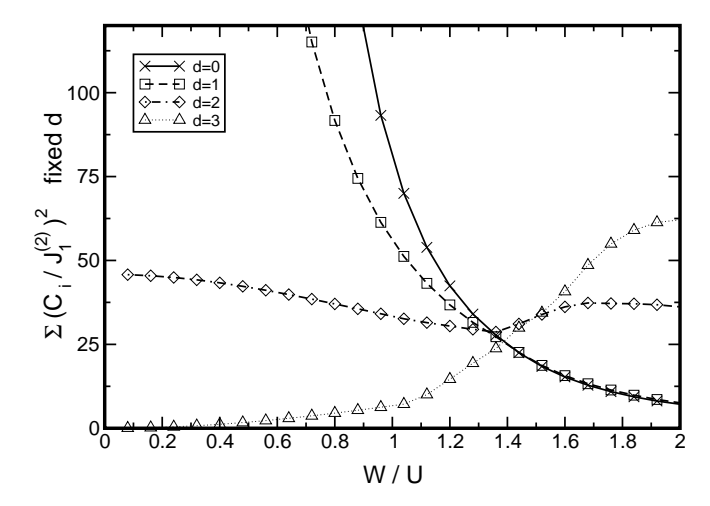


FIG. 7: Distribution of coefficients as function of W/U according to the spatial extension d of the respective terms in the double-plaquette calculation (v). The sum of the squares of the coefficients are plotted relative to the second order Heisenberg exchange  $J_1^{(2)}=4t^2/U$ .

Next, we analyze the distribution of coefficients over operators of various extensions d, see Sect. III, and the effect of truncating the proliferating terms. Fig. 7 shows the sum of the squares of all coefficients  $C_i$  of terms with the definite extension d at the end of the flow. They are given as functions of W/U. The results are given in units of  $J_1^{(2)} = 4t^2/U$  which is a natural scale for the parameters defining the effective model. The only operator with extension zero is the Hubbard repulsion term  $H_U$ . For increasing W/U the relevance of the most local terms with d=0 and d=1 decreases, whereas terms with larger extension become more and more important. Note especially the increase of the coefficients of the operators with maximal extension d=3.

The distribution of coefficients indicates that up to  $W/U \approx 1.2$  all important operators are included in our calculation. Beyond  $W/U \gtrsim 1.2$  the coefficients with extension d=3 become more important. Thus terms with larger extension would have sizeable coefficients and should be taken into account. This indicates that the approximations become definitely insufficient beyond  $W/U \gtrsim 1.2$ .

To obtain clearer information on the applicability of the mapping and on the accuracy of the approximations we examine the apparent charge gap  $\Delta_{\rm app}$ . To this end, the dispersion  $E_k$  of a single DO moving in the paramagnetic spin background is determined by a Lanczos calculation<sup>25,26</sup>. In this calculation we treat the operators as vectors as in the projection technique<sup>27</sup>. The effective Hamiltonian acts by commutation as a superoperator on the operators. This is conveniently denoted by the Liouville operator  $\mathcal{L} := [H, \cdot]$ . The "scalar product" (A|B) is defined by  $\text{Tr}(A^{\dagger}B\hat{\rho}_0)$  relative to the paramagnetic reference ensemble (6). Note that this scalar

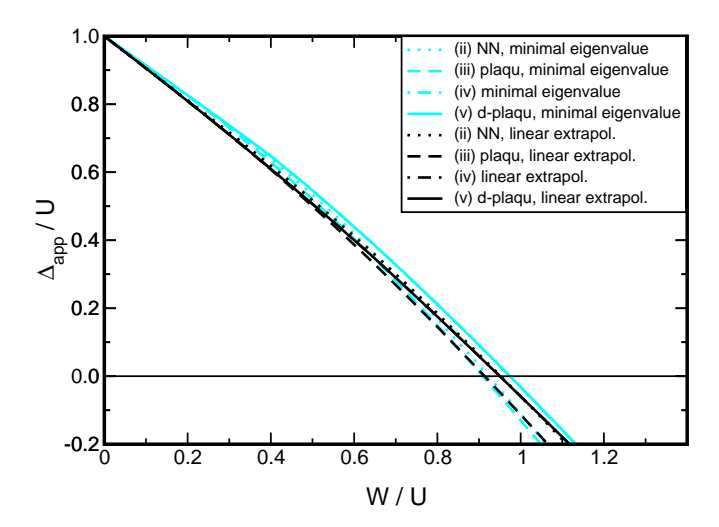


FIG. 8: Apparent charge gap as calculated with Lanczos diagonalization. Grey lines show the minimal eigen values, black lines the result of a linear extrapolation.

product is only positive semi-definite since there can be operators whose norm vanishes.

The projection formalism is the appropriate concept for this calculation since we are not dealing with simple states in a Hilbert space but with ensembles which are derived from the paramagnetic one (6) by the application of operators. These operators induce deviations from the reference ensemble which constitute excitations. As usual in the Heisenberg picture, the dynamics of operators in the frequency domain is captured by the commutation with the Hamiltonian.

We start the Lanczos approach from the operator  $\mathcal{O}_0$ which generates a single DO with momentum k

$$\mathcal{O}_0 := \frac{1}{\sqrt{N}} \sum_{\mathbf{r}} e^{i\mathbf{k}\mathbf{r}} n_{\mathbf{r},\downarrow} c_{\mathbf{r},\uparrow}^{\dagger} \tag{19}$$

where the number of sites is denoted by N and the sum extends over the whole lattice. A set of orthogonal operators is generated by the iterative application of  $\mathcal{L}$ 

$$\mathcal{O}_{n+1} = \mathcal{L}\mathcal{O}_n - a_n \mathcal{O}_n - b_n^2 \mathcal{O}_{n-1} , \qquad (20)$$

where

$$a_n = (\mathcal{O}_n | \mathcal{L} \mathcal{O}_n) / (\mathcal{O}_n | \mathcal{O}_n) , \qquad (21a)$$
  
$$b_{n+1}^2 = (\mathcal{O}_{n+1} | \mathcal{O}_{n+1}) / (\mathcal{O}_n | \mathcal{O}_n), \quad b_0 = 0 . (21b)$$

$$b_{n+1}^2 = (\mathcal{O}_{n+1}|\mathcal{O}_{n+1})/(\mathcal{O}_n|\mathcal{O}_n), \quad b_0 = 0.$$
 (21b)

Note that the application of  $\mathcal{L}$  derived from the effective Hamiltonian after the CUT does not change the number of DOs. Hence its action on the initial vector is (i) to shift the DO and/or (ii) to change the spin background. The iteratively built basis  $\{\mathcal{O}_n\}$  describes a single DO (charge excitation) at momentum **k** including its magnetic dressing. In this basis the Liouville operator is a tridiagonal matrix where the  $a_n$  are the diagonal matrix elements and the  $b_n$  are the elements on the secondary diagonal.

The lowest energy in this subspace defines the (apparent) dispersion  $E_k$  of a single charge excitation relative to the paramagnetic ensemble. Hence the evaluation of the lowest accessible energy in any truncated subspace of  $\{\mathcal{O}_n\}$  provides an upper bound to  $E_k$ . The apparent charge gap  $\Delta_{\rm app}$  is finally given by

$$\Delta_{\rm app} = 2 \min_k E_k \ , \tag{22}$$

where the factor of 2 is put to account for the creation of a particle and a hole. For vanishing hopping  $\Delta_{app} = U$ holds. The apparent charge gap  $\Delta_{\rm app}$  is not the true charge gap because the paramagnetic spin background is not the true ground state. But  $\Delta_{app}$  is a measure of the separation of energies between sectors of different double

Numerically, one has to restrict the above procedure to truncated basis sets. In practice, we construct a sequence of basis sets, labelled by the integer n, by applying the Liouville operator  $\mathcal{L}_0 := [T_0, \cdot]$  (cf. Eq. 4b) iteratively to the initial operator (19). The first basis n = 1 consists only of the single operator  $\mathcal{O}_0$ . The subsequent basis sets are generated by applying  $T_0$  (n-1) times. All the components which are products of the local operators in Tab. I are treated as independent vectors of the basis. For each basis set the lowest eigen value of the matrix representation of the Hamiltonian in this basis yields an upper bound to the lowest energy  $E_k$  of a single DO.

The calculation was done for k-values on the high symmetry lines in **k**-space from  $(0,0)-(\pi/a,\pi/a)-(\pi/a,0)-$ (0,0). Figure 8 shows the results of the Lanczos calculation. The computational effort grows with the number of terms in the Hamiltonian. For the effective Hamiltonians (iv) and (v) it was only possible to do the calculation up to the basis set n = 6, whereas for the NN (ii) and plaquette (iii) Hamiltonians the n=7 calculation was feasible. In Fig. 8 grey lines show the smallest eigen value found for all momenta k in the largest possible Lanczos calculation. An additional estimate for the gap is found by extrapolating the lowest eigen values at momentum  $(\pi/a, \pi/a)$  for each basis set as function of 1/n to  $n \to \infty$ .

The lowest eigen value at momentum  $(\pi/a, \pi/a)$  is usually also the minimum of the dispersion except for n=5,6 or 7 where the whole dispersion becomes very flat. The result from a fit linear in 1/n is included in Fig. 8 by black lines. For the minimal eigen values as well as for the extrapolated ones the result for the Hamiltonian (iv) is covered by the double-plaquette result (v), since the coefficients of the Hamiltonians nearly coincide. The lowest eigen values for the Hamiltonians (iv) and (v) are larger than the lowest eigen values for the Hamiltonians (ii) and (iii) because larger values of n were accessible for the latter.

A first guess for the gap is  $\Delta_{app}/U = 1 - W/U$ , see e.g. Ref. 8. So one expects that the gap closes around W/U = 1. The apparent charge gap calculated within the effective model using Lanczos-diagonalization displays a similar behavior. The gap decreases almost linearly from  $\Delta_{\rm app}/U=1$  at W/U=0. There is, however, a certain downward curvature so that it closes at about  $W/U\approx 0.9$ . Taking into account even larger basis sets might further lower the ratio W/U where the gap closes. The linear extrapolation corroborates the results from the linear eigen values to a certain extent. But we could not identify a clear asymptotic behaviour for large values of n. Other extrapolation schemes, for instance as function of  $1/\sqrt{n}$ , point towards an earlier closing of the apparent charge gap. Therefore the value  $W/U\approx 0.9$  for the closing of the gap must be seen as a rough estimate. The determination of the power law by which the gap closes is beyond the scope of the present paper.

The above findings are discussed in more detail in Sect. V. In the sequel, we have to keep in mind that the mapping to the effective model conserving the number of DOs is not possible for  $W/U \gtrsim 0.9$ . For completeness, we will present the coefficients of the generalized t-J model up to values W/U = 1.6 to illustrate in which way the results are affected by the breakdown of the mapping. As a reminder of the breakdown, the definitely unphysical region beyond  $W/U \approx 1$  will be shaded in the figures.

# B. Effective spin model

Strictly at half-filling, the effective model can be cast into the form of a pure spin Hamiltonian. There are various two-spin couplings of the Heisenberg-type

$$H_{2\text{-spin}} = \sum_{i,j} J_{|j-i|} \mathbf{S}_i \cdot \mathbf{S}_j. \tag{23}$$

This type of exchange may exist for sites i and j of any distance but it is of course largest for adjacent sites. Fig. 9 displays the coefficients of various two-spin couplings. The Heisenberg NN exchange  $J_1$  is shown in Fig. 9a, the exchange couplings between second and third nearest neighbors,  $J_2$  and  $J_3$ , are depicted in Fig. 9b and 9c, respectively. The coefficients are shown relative to  $J_1^{(2)}=4t^2/U$ . The coupling  $J_1$  is only renormalized slightly to lower values  $\approx 0.92J_1^{(2)}$  for W/U=1 contrary to what one might have expected from the strong influence of higher terms in perturbation theory. Already the NN calculation reproduces the leading order correctly and yields a very reasonable result for larger values of W/U, see also Fig. 4 and the discussion thereof. The convergence of the various calculations shows that the terms retained are sufficient to determine  $J_1$  to very good accuracy. Note that the dotted curve of the plaquette calculation (iii) is almost hidden by the double-plaquette result (v).

The couplings  $J_2$  and  $J_3$  behave like  $(t/U)^4$  for small W/U. Their absolute convergence is as good as for  $J_1$ . But due to their small values – both are smaller than  $0.02J_1^{(2)}$  for W/U < 1 – the relative differences between calculations on different clusters are still discernible.

There are not only exchange terms between two spins but also between four or more spins. Exchange between

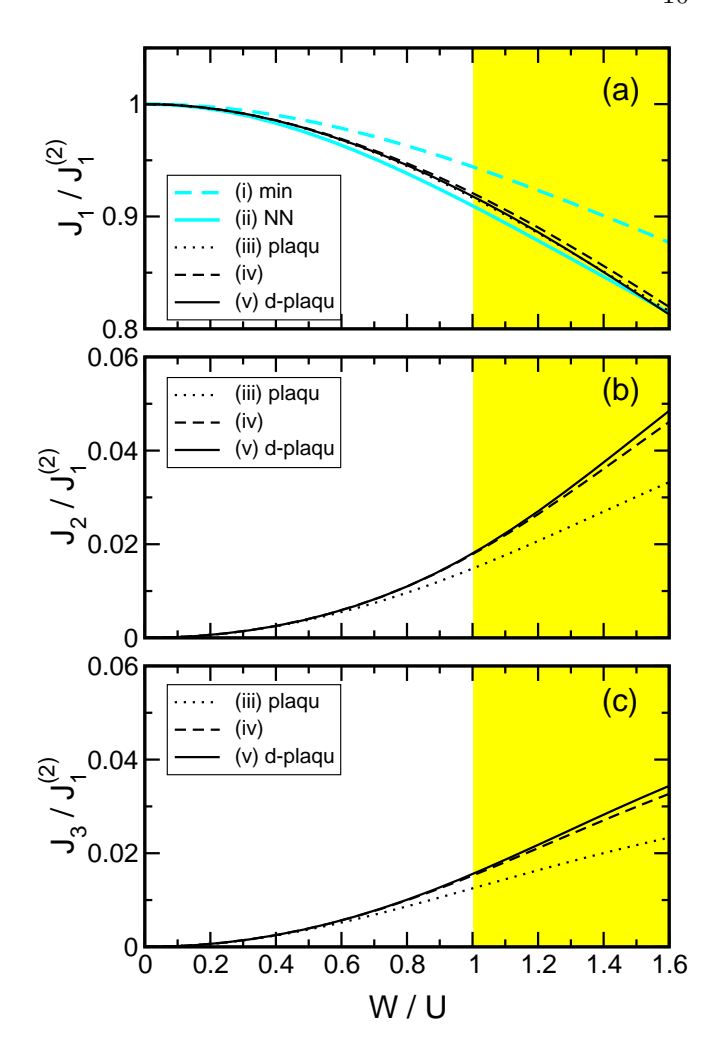


FIG. 9: Couplings of two-spin operators relative to  $J_1^{(2)}$  as function of W/U.

an odd number of spins is not generated since such terms would change sign under time reversal. The first term that one encounters in perturbation theory<sup>3</sup> in 4th order is the four-spin part of the ring-exchange which takes the form

$$H_{\square} = J_{\square} \sum_{\langle i,j,k,l \rangle} \left[ (\mathbf{S}_{i} \cdot \mathbf{S}_{j})(\mathbf{S}_{k} \cdot \mathbf{S}_{l}) + (\mathbf{S}_{i} \cdot \mathbf{S}_{l})(\mathbf{S}_{j} \cdot \mathbf{S}_{k}) - (\mathbf{S}_{i} \cdot \mathbf{S}_{k})(\mathbf{S}_{j} \cdot \mathbf{S}_{l}) \right]$$
(24)

where  $\langle i,j,k,l \rangle$  label the sites around a plaquette of the square lattice in cyclic order. In 6th order an additional independent four-spin operator reads

$$H_{\times} = J_{\times} \sum_{\langle i,j,k,l \rangle} (\mathbf{S}_i \cdot \mathbf{S}_k) (\mathbf{S}_j \cdot \mathbf{S}_l).$$
 (25)

The coefficients  $J_{\square}$  and  $J_{\times}$  are plotted in Figs. 10a and 10b. The ring exchange  $J_{\square}$  is the most important modification of the pure NN Heisenberg model. Its value

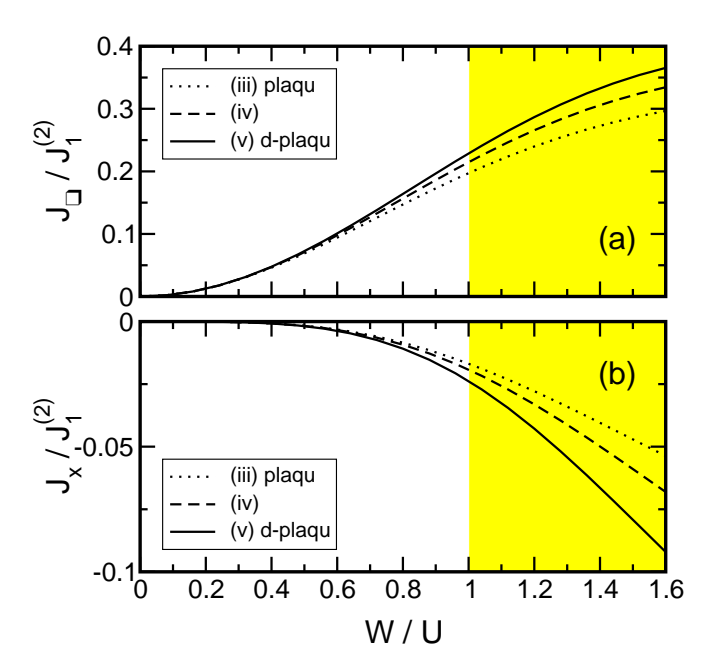


FIG. 10: Couplings of four-spin operators relative to  $J_1^{(2)}$  as function of W/U.

is larger than  $0.2J_1^{(2)}$  for W/U=1. The relevance of the ring-exchange was also confirmed experimentally in the CuO<sub>2</sub>-planes of La<sub>2</sub>CuO<sub>4</sub><sup>28</sup> and theoretically in the derivation of the effective spin model from a three-band model<sup>29,30,31</sup>. The influence of ring-exchange on the Raman line shape was computed in spin wave theory<sup>32</sup>.

It is worth noting that the coefficients of the effective spin model are smooth functions of W/U up to W/U=1.6. The vanishing of the apparent gap  $\Delta_{\rm app}$  and the slow drop of the residual off-diagonality for  $W/U\gtrsim 1$  do not give rise to an anomalous behavior of the effective spin coefficients. The convergence of the results for values  $W/U\lesssim 1$  is very good, i.e., the couplings do not change much as function of the cluster size for the larger clusters.

### C. Effective charge model

The unitary transformation deals also with the motion and interaction of charges. In the course of the transformation charge excitations (DOs) are created virtually. After the transformation, DOs can be introduced externally by doping or thermal fluctuations. Note that generically the effective model displays a finite U term. So DOs are not suppressed. But due to the disentanglement of the sectors of different number of DOs there is no direct influence of these sectors on one another. For instance, the magnetism strictly at half-filling is not influenced by the physics of the sector with a particle-hole pair (two DOs in our counting).

But thermal expectation values are generically influenced by the presence of sectors of different number of DOs. Also spectral properties are influenced by the presence of these sectors. The spectral weight will be distributed over a number of sectors. There are Hubbard bands beyond the lower (one hole) and the upper (one electron) Hubbard band, for instance a trans-upper Hubbard band characterized by two electrons and a hole relative to the paramagnetic reference ensemble. But preliminary estimates of the spectral weight in this band indicate that it is below the order of one percent. Yet it is a strong point of the approach chosen that the concept allows to discuss such subtle effects.

In the present paper, we focus on the effective Hamiltonian leaving the determination of spectral weights to future work. We will present the results for the most important terms concerning the dynamics of charges. In order not to be lost in a proliferating number of terms we will present results for terms which are at most of order  $t^2/U$  in the limit of weak hopping.

First, we address the terms which move a single DO, i.e. various hopping processes. Besides the NN hopping  $T_0$ , the next relevant hopping processes are those between next-nearest neighbor (NNN) sites and third-nearest neighbor sites (3NN). The NNN sites lie on diagonally opposite corners of the plaquettes of the two-dimensional square lattice. All hopping processes and interactions that appear in second order in t/U will be shown. The NNN hopping  $T_0'$  reads

$$T_0' = t' \sum_{\langle\langle i,j\rangle\rangle;\sigma} \left[ (1 - n_{i,\sigma}) c_{i,\overline{\sigma}}^{\dagger} c_{j,\overline{\sigma}} (1 - n_{j,\sigma}) - n_{i,\sigma} c_{i,\overline{\sigma}}^{\dagger} c_{j,\overline{\sigma}} n_{j,\sigma} + \text{h.c.} \right]$$
(26)

where  $\langle \langle i, j \rangle \rangle$  stands for NNN sites and  $\overline{\sigma} = -\sigma$ . The spin-dependent NNN hopping  $T'_{s,0}$  reads

$$T'_{s,0} = t'_{s} \sum_{\langle i,k,j \rangle; \alpha,\beta} \left\{ \left[ (1 - n_{i,\alpha}) c_{i,\overline{\alpha}}^{\dagger} \boldsymbol{\sigma}_{\overline{\alpha},\overline{\beta}} c_{j,\overline{\beta}} (1 - n_{j,\beta}) \right] \cdot \mathbf{S}_{k} + \left[ n_{i,\alpha} c_{i,\overline{\alpha}}^{\dagger} \boldsymbol{\sigma}_{\overline{\alpha},\overline{\beta}} c_{j,\overline{\beta}} n_{j,\alpha} \right] \cdot \mathbf{S}_{k} + \text{h.c.} \right\}$$
(27)

where  $\langle i,k,j \rangle$  stands for three sites wherein i and j are NNN and k is a nearest neighbor to both i and j. The symbol  $\boldsymbol{\sigma}=(\sigma_x,\sigma_y,\sigma_z)$  stands for the vector made out of the three Pauli-matrices;  $\mathbf{S}_k$  represents the usual S=1/2 spin vector at site k. Hopping and spin-dependent hopping between 3NN is also produced in second order in t/U. They read

$$T_0'' = t'' \sum_{\langle\langle\langle\langle i,j\rangle\rangle\rangle;\sigma} \left[ (1 - n_{i,\sigma}) c_{i,\overline{\sigma}}^{\dagger} c_{j,\overline{\sigma}} (1 - n_{j,\sigma}) - n_{i,\sigma} c_{i,\overline{\sigma}}^{\dagger} c_{j,\overline{\sigma}} n_{j,\sigma} + \text{h.c.} \right]$$
(28)

where  $\langle \langle \langle i, j \rangle \rangle \rangle$  stands for 3NN sites and

$$T_{s,0}'' = t_s'' \sum_{\langle\langle i,k,j\rangle\rangle;\alpha,\beta} \left\{ \left[ (1 - n_{i,\alpha}) c_{i,\overline{\alpha}}^{\dagger} \boldsymbol{\sigma}_{\overline{\alpha},\overline{\beta}} c_{j,\overline{\beta}} (1 - n_{j,\beta}) \right] \cdot \mathbf{S}_k + \left[ n_{i,\alpha} c_{i,\overline{\alpha}}^{\dagger} \boldsymbol{\sigma}_{\overline{\alpha},\overline{\beta}} c_{j,\overline{\beta}} n_{j,\alpha} \right] \cdot \mathbf{S}_k + \text{h.c.} \right\}$$
(29)

where  $\langle \langle i, k, j \rangle \rangle$  stands for three sites wherein i and j

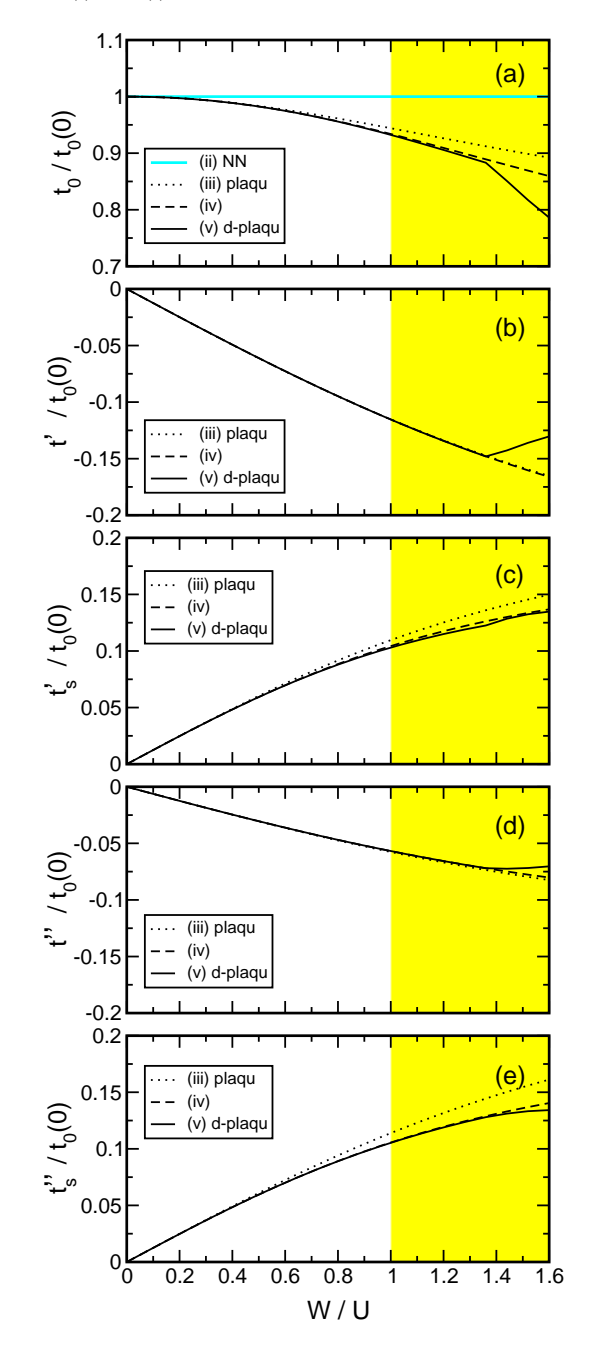


FIG. 11: Effective hopping coefficients between (a) NN sites, (b) NNN sites, (c) spin-dependent NNN hopping, (d) 3NN sites and (e) spin-dependent 3NN hopping.

are 3NN and k is a nearest neighbor to both i and j, so k is just the site between i and j. All these hoppings

(26)-(29) conserve the number of DOs. Figs. 11a-e show the coefficients of the NN hopping  $t_0$  ( $T_0$  from Eq. (4b)), NNN hopping t', spin-dependent NNN hopping  $t'_s$ , 3NN hopping t'' and spin-dependent 3NN hopping  $t''_s$ , respectively. They are shown in units of the unrenormalized value  $t_0(0) = t$  for the NN hopping.

The NN hopping  $t_0$  shown in Fig. 11a remains unchanged from its initial value for the NN truncation. Including more terms reduces the effective  $t_0$ . At  $W/U \approx$ 1.36, the double plaquette calculation (v) shows a sudden change of slope. This is related to the non-monotonic behavior of the residual off-diagonality. But the value  $W/U \approx 1.36$  is already beyond the point  $W/U \approx 0.9$ where the apparent gap  $\Delta_{\rm app}$  becomes negative and the mapping is no longer possible. The signs of t' (NNN hopping) and of t'' (3NN hopping) are opposite to the sign of t (NN hopping). The value of t' is approximately two times t'' because it is generated from the two possible hopping processes to go from one corner of a plaquette to the opposite corner. In contrast, there is only one process to generate t'' in second order. The results for the calculations (iii)-(v) lie almost on top of each other for the coefficients t, t' and t'' until spurious behavior sets in at larger values of W/U.

Figures 12 and 13 show the coefficients for terms that describe interactions between charges. In Fig. 12a, the Hubbard repulsion U is shown in units of its unrenormalized value. All calculations show a slight increase of the effective U with W/U. It is interesting to note that this basic quantity neither diverges nor stays constant in the process of the disentanglement of the various sectors of double occupancy.

All processes discussed in the sequel have the property to be active only if at least two DOs are present. In our counting this means that at least two holes or two doubly occupied sites or one hole and one doubly occupied site must be present. In this sense, the following processes represent two-particle interactions. The density-density interactions for NN sites is described by

$$H_V = V \sum_{\langle i,j \rangle} \bar{n}_i \bar{n}_j \tag{30}$$

where  $\bar{n}_i = n_{i,\uparrow} + n_{i,\downarrow} - 1$ . Similarly, the operator for

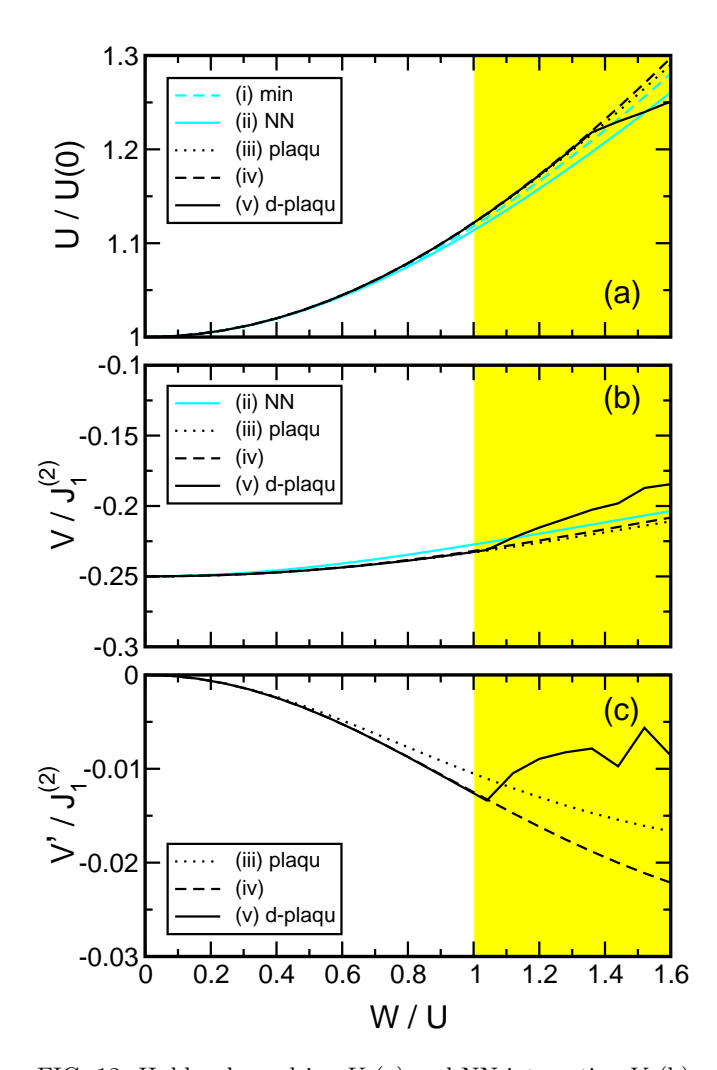


FIG. 12: Hubbard repulsion U (a) and NN interaction V (b) and NNN interaction V' (c) between holes or double occupancies.

density-density interactions for NNN sites reads

$$H_{V'} = V' \sum_{\langle \langle i,j \rangle \rangle} \bar{n}_i \bar{n}_j.$$
 (31)

The coefficients V and V' are shown in Fig. 12b and 12c. They are given in units of the second order scale  $J_1^{(2)} = 4t^2/U$ . The attractive interaction V is proportional to  $-t^2/U = -J_1^{(2)}/4$  as expected from perturbation theory. It represents a sizeable contribution at all W/U. In contrast, the V' coupling NNN sites, which is of fourth order in t/U, turns out to be very small<sup>33</sup>. This fact justifies our choice to focus otherwise on the terms which appear already in second order in t.

There are two additional types of operators that are created in second order in t/U. The first type consists of operators which destroy or create two electrons at the

same site. Figure 13a shows the coefficient  $V_{\rm pair}$  of

$$H_{\text{pair}} = V_{\text{pair}} \sum_{\langle i,j \rangle} c_{i,\uparrow}^{\dagger} c_{i,\downarrow}^{\dagger} c_{j,\downarrow} c_{j,\uparrow}. \tag{32}$$

Figure 13b and c show the coefficients  $V'_{\text{pair}}$  and  $V''_{\text{pair}}$  of

$$H'_{\text{pair}} = V'_{\text{pair}} \sum_{\langle i, k, j \rangle, \sigma} \left[ c^{\dagger}_{k, \sigma} c^{\dagger}_{k, \bar{\sigma}} c_{i, \bar{\sigma}} n_{i, \sigma} c_{j, \sigma} (1 - n_{j, \bar{\sigma}}) + c^{\dagger}_{k, \sigma} c^{\dagger}_{k, \bar{\sigma}} c_{i, \bar{\sigma}} (1 - n_{i, \sigma}) c_{j, \sigma} n_{j, \bar{\sigma}} + \text{h.c.} \right], \quad (33)$$

$$H''_{\text{pair}} = V''_{\text{pair}} \sum_{\langle \langle i, k, j \rangle \rangle, \sigma} \left[ c^{\dagger}_{k, \sigma} c^{\dagger}_{k, \bar{\sigma}} c_{i, \bar{\sigma}} n_{i, \sigma} c_{j, \sigma} (1 - n_{j, \bar{\sigma}}) + c^{\dagger}_{k, \sigma} c^{\dagger}_{k, \bar{\sigma}} c_{i, \bar{\sigma}} (1 - n_{i, \sigma}) c_{j, \sigma} n_{j, \bar{\sigma}} + \text{h.c.} \right]. \quad (34)$$

The operators  $H'_{\mathrm{pair}}$  and  $H''_{\mathrm{pair}}$  describe processes where two electrons from sites i and j are transferred to site k. They do not change the number of DOs since at one site (with local operator  $c_{i,\sigma}(1-n_{i,\bar{\sigma}})$ ) a DO is created while at another  $(c_{i,\sigma}n_{i,\bar{\sigma}})$  a DO is annihilated. The local operator  $c_{k,\uparrow}^{\dagger}c_{k,\downarrow}^{\dagger}$  turns an empty site into a doubly occupied site and thus does not change the number of DOs in our counting. Both the coefficients  $V'_{\mathrm{pair}}$  and  $V''_{\mathrm{pair}}$  change only slightly on passing from calculation (iii) to calculation (iv); the difference between (iv) and (v) is minute so that we consider the final result as reliable for not too large W/U where the mapping to the generalized t-J models is possible.

The last type of operators created in second order in t/U are correlated hopping terms. We classify them as interactions because they have a non-vanishing effect only if at least two double occupancies or holes are present. The operator

$$V'_{n,0} = V'_{n} \sum_{\langle i,k,j\rangle;\alpha,\beta} \left[ (1 - n_{i,\alpha}) c_{i,\overline{\alpha}}^{\dagger} c_{j,\overline{\beta}} (1 - n_{j,\beta}) \bar{n}_{k} + n_{i,\alpha} c_{i,\overline{\alpha}}^{\dagger} c_{j,\overline{\beta}} n_{j,\beta} \bar{n}_{k} + \text{h.c.} \right]$$
(35)

describes a process of a DO hopping between the NNN sites i and j if and only if there is a DO on the site k. The corresponding operator for a 3NN process is

$$V_{n,0}^{"} = V_{n}^{"} \sum_{\langle\langle i,k,j\rangle\rangle;\alpha,\beta} \left[ (1 - n_{i,\alpha}) c_{i,\overline{\alpha}}^{\dagger} c_{j,\overline{\beta}} (1 - n_{j,\beta}) \bar{n}_{k} + n_{i,\alpha} c_{i,\overline{\alpha}}^{\dagger} c_{j,\overline{\beta}} n_{j,\beta} \bar{n}_{k} + \text{h.c.} \right].$$
(36)

The coefficients  $V'_n$  and  $V''_n$  are shown in Fig. 13d and e.

The above results define the charge dynamics of the t-J model in a systematic and exhaustive way. We highlight the importance of spin-dependent hoppings. All the values for the hopping coefficients and the interactions show excellent convergence in the relevant region up to  $W/U \approx 0.9$ . We find again that for values W/U > 0.9 the coefficients display anomalous behavior. This effect is most striking for the coefficient V' in Fig. 12c.

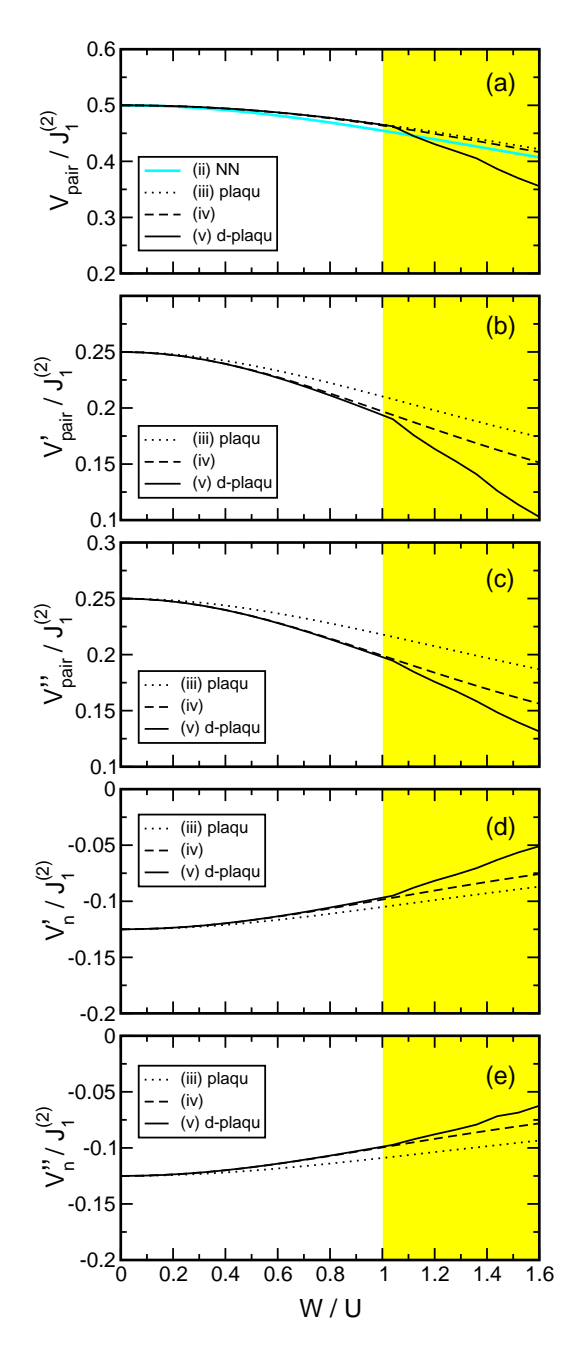


FIG. 13: Further coefficients of interactions of two DO that are of second order in t/U. For explanation, see text.

We attribute this spurious behavior to the breakdown of the mapping of the Hubbard model to a generalized t-Jmodel without specifying the state of the spin degrees of freedom.

#### V. DISCUSSION

In this section, we will discuss the physical significance of our findings for the square lattice and compare them to the situation for the Hubbard model in infinite dimensions.

In the derivation of the effective t-J-model, one does not aim at the solution of the complete problem of the Hubbard model on the square lattice. The CUT is designed to disentangle the energetically low-lying dynamics, i.e., the dynamics of the spins and of the doped holes, from processes involving more double occupancies. So no particular state in spin space is assumed, but an effective model without processes changing the number of double occupancies is derived. In this calculation, the paramagnetic ensemble at half-filling serves as reference ensemble.

The general consideration presented in the Introduction suggested that the reduction to the effective model without charge fluctuations cannot be defined for too large W/U. Our findings fully corroborate this view. The reduction of the Hubbard model to a generalized t-J model is possible as long as the apparent gap  $\Delta_{\rm app}$  remains non-negative. The appearance of negative values for  $\Delta_{\rm app}$  is an artefact. It indicates that the paramagnetic reference ensemble does no longer represent a phase which is stable against fluctuations involving double occupancies. In this case the reduction to an effective model without virtual double occupancies is no longer possible.

The concept of the apparent gap is introduced as a quantitative measure of the energetic separation of the low-lying degrees of freedom from the fluctuations involving double occupancies. But it is not easy to visualize since it does not refer to true eigen states of the system. So it is helpful for a qualitative understanding to consider a modified system where the apparent and the true gap coincide. This situation is realized for a Hubbard model on the Bethe lattice in the limit of infinite coordination number  $Z \to \infty$ , cf. Refs. 8,9,10,34. For infinite dimensional lattices it is assumed that long-range order can be completely suppressed by frustration, e.g., in the generalizations of fcc lattices to infinite dimensions<sup>35,36</sup>. Since the magnetic couplings J scale with the inverse coordination number  $Z^{-1}$  there are no magnetic correlations at all once the static sublattice magnetization is suppressed<sup>37</sup>. This is so since the second moment of the magnetic couplings, averaged over adjacent sites, vanishes in the limit  $Z \to \infty$ . There is even no nearest-neighbor correlation. Hence the paramagnetic reference ensemble represents the highly degenerate magnetic ground state in infinite dimensions without long-range order. The apparent gap and the true charge gap are identical. Their closure signals a real insulator-to-metal transition. In finite dimensions the closure of the apparent gap signals only a crossover from well-separated to non-separated energy

We see that the (paramagnetic) insulator-to-metal crossover in finite dimensions can be studied in the purified form of a phase transition in the infinite dimensional Hubbard model. Indeed, similar behavior is found. The single-particle gap  $\Delta$  vanishes in infinite dimensions at about  $1.1W - 1.2W^{10,34,38,39,40}$ . It disappears roughly linearly as function of  $U^{10,34}$ . These similarities corroborate the infinite dimensional model as illustration for the

crossover in finite dimensions.

The validity of our approach is clear for small values of W/U. The only approximation used is the truncation of processes of a spatial range  $d \geq 4$ . The remaining question is to know up to which ratio of W/U the results are reliable. Our findings in finite dimensions illustrate that the answer to this question is difficult already on the conceptual level. The apparent gap  $\Delta_{\rm app}$  measuring the separation of energy scales does not compare the energies of real eigen states. Hence we claim that the validity of the mapping of the Hubbard model to a generalized t-Jmodel is not limited by a sharply defined transition but by a gradual crossover.

An estimate up to which ratio of W/U the mapping is reasonable can be obtained from the closure of the apparent gap at around  $W/U \approx 0.9$ . A better estimate for the region of validity should compare  $\Delta_{app}$  to the size of the coefficients of the neglected operators. But these coefficients are not available. Hence we compare  $\Delta_{\rm app}$  to the size of the coefficients of the operators with the maximal extension considered, that is d=3. Both energies become equal for  $W/U \approx 0.85$ . If in addition we take the uncertainty of the extrapolation procedure into account we arrive at the conservative estimate that the generalized t-J model can be used up to  $W/U \approx 0.8$ which includes the commonly assumed parameters for cuprate planes  $t/J \approx 3$  which translates to  $W/U \approx 0.7$ . Up to  $W/U \approx 0.8$ , the quantitative results provided in this article are reliable.

In conclusion, we find that the possibility to map a Hubbard model in a systematic and controlled way to a generalized t-J model depends essentially on local physics. We stress, however, that the breakdown of this mapping does not represent a real physical phase transition in finite dimensions. We suppose that the breakdown of the mapping manifests itself in physical properties as a crossover. It is plausible, for instance, that the nature of the elementary excitations changes: holes and magnetic modes for large values of the interaction become fermionic quasi-particles at small values of the interaction.

## VI. SUMMARY

We introduced a self-similar CUT to map the Hubbard model at strong coupling onto an effective model. The generator of the transformation is chosen such that the number of double occupancies is conserved by the effective model which is thus a generalized t-J model. The CUT allows to do this in a systematic and nonperturbative way which includes the dynamics of doped holes as well as the spin dynamics. Thus our analysis extends previous ones in two important aspects: the nonperturbative treatment of the couplings and the systematic treatment of the dynamics of doped charge carriers.

The calculations confirmed our expectations which were based on qualitative arguments. The fundamental

result is that for  $U\gtrsim 1.3W$  the mapping of the Hubbard model to a generalized t-J model is possible. The parameters of the effective model can be determined reliably by the CUT. They are governed mainly by local physics. On the other hand, the reduction of the Hubbard model to an effective model without charge fluctuations is not possible for  $U \lesssim 1.2W$ . Here, the sectors of different number of double occupancies cannot be disentangled.

The truncation scheme necessary to close the flow equation of the CUT was based on the extension of the operators. In order to define the extension of an operator a physically meaningful unique notation is required. This was achieved by introducing a normal-ordering with respect to a vacuum. The vacuum chosen here was the paramagnetic ensemble without any magnetic correlations.

Besides the NN Heisenberg exchange further two-spin terms and four-spin terms were taken into account. It was shown that two-spin couplings other than the Heisenberg term are small whereas the four-spin ring exchange  $J_{\square}$  gives a sizeable contribution to the effective spin model. Results for the size of the coefficients for NN hopping, NNN hopping and spin-dependent NNN hopping were obtained. It was found that the spin-dependent NNN and 3NN hopping is as important as the spinindependent one. We recommend to account for this fact in phenomenological parametrizations of experimental Fermi surfaces. In addition, the size of the interactions between holes and double occupancies on NN and NNN sites were calculated. Various truncation schemes show very good convergence of the coefficients of the effective model in the relevant parameter region  $W \leq 0.8U$ .

Our results suggest that self-similar continuous unitary transformations can be used also for other models, e.g. more realistic multi-band Hubbard models, in order to achieve a systematic and quantitative reduction to effective models.

## Acknowledgments

We thank K.P. Schmidt for stimulating discussions and the DFG for financial support in SFB 608.

## APPENDIX A: THE NN TRUNCATION

To carry out the CUT with all operators on NN sites the terms (12c) and (12d) in equation (12) have to be included in the Hamiltonian

$$H_V = V(\ell) \sum_{\langle i,j \rangle} \bar{n}_i \bar{n}_j$$
 (A1)

$$H_{V} = V(\ell) \sum_{\langle i,j \rangle} \bar{n}_{i} \bar{n}_{j}$$

$$H_{\text{pair}} = V_{\text{pair}}(\ell) \sum_{\langle i,j \rangle} c_{i,\uparrow}^{\dagger} c_{i,\downarrow}^{\dagger} c_{j,\downarrow} c_{j,\uparrow} .$$
(A1)

 $H_V$  describes interactions of electrons on NN sites,  $H_{\text{pair}}$ the hopping of two electrons between site i and j. These terms do not change the number of DOs. Thus, they generate no new contributions in  $\eta$ . Calculating  $[\eta, H_{\rm NN} + H_V + H_{\rm pair}]$  and neglecting again terms that do not fit on NN sites we obtain the closed flow equation

$$d_{\ell}U(\ell) = 32t_{+2}(\ell)^2 \tag{A3a}$$

$$d_{\ell}t_0(\ell) = 0 \tag{A3b}$$

$$d_{\ell}t_{+2}(\ell) = -2U(\ell)t_{+2}(\ell)$$

$$+t_{+2}(\ell) (2V(\ell) - 2V_{\text{pair}}(\ell) - 3J(\ell)/2))$$
(A3c)

$$d_{\ell}J_{1}(\ell) = 16t_{+2}(\ell)^{2} \tag{A3d}$$

$$d_{\ell}V(\ell) = -4t_{+2}(\ell)^2 \tag{A3e}$$

$$d_{\ell}V_{\text{pair}}(\ell) = 8t_{+2}(\ell)^2 . \tag{A3f}$$

The solution for  $J_1$  is

$$J_1^{\text{NN}}(\ell) = \frac{2r}{7} \tanh(2r\ell + D) - \frac{2}{7}U_0$$
 (A4)

where  $r=\sqrt{28t_0^2+{U_0}^2}$  and  $D=\mathrm{arctanh}(U_0/r)$ . This yields in the limit  $\ell\to\infty$  the effective NN spin-coupling of the NN truncation

$$J_{1,\text{eff}}^{\text{NN}} = \frac{2}{7}\sqrt{U^2 + 28t^2} - \frac{2}{7}U$$
, (A5)

where the final result is given in the bare parameters recalling  $t_0 = t, U_0 = U$ .

<sup>&</sup>lt;sup>1</sup> P. W. Anderson, Phys. Rev. **115**, 2 (1959).

<sup>&</sup>lt;sup>2</sup> D. J. Klein and W. A. Seitz, Phys. Rev. B 8, 2236 (1973).

<sup>&</sup>lt;sup>3</sup> M. Takahashi, J. Phys. C **10**, 1289 (1977).

<sup>&</sup>lt;sup>4</sup> A. B. Harris and R. V. Lange, Phys. Rev. **157**, 295 (1967).

<sup>&</sup>lt;sup>5</sup> A. H. MacDonald, S. M. Girvin, and D. Yoshioka, Phys. Rev. B 37, 9753 (1988).

<sup>&</sup>lt;sup>6</sup> J. Stein, J. Stat. Phys. **88**, 487 (1997).

<sup>&</sup>lt;sup>7</sup> E. H. Lieb and F. Y. Wu, Phys. Rev. Lett. **20**, 1445 (1968).

<sup>&</sup>lt;sup>8</sup> F. Gebhard, The Mott Metal-Insulator Transition, Vol. 137 of Springer Tracts in Modern Physics (Springer, Berlin, 1997).

<sup>&</sup>lt;sup>9</sup> A. Georges, G. Kotliar, W. Krauth, and M. J. Rozenberg, Rev. Mod. Phys. 68, 13 (1996).

M. P. Eastwood, F. Gebhard, E. Kalinowski, S. Nishimoto, and R. M. Noack, Eur. Phys. J. B 35, 155 (2003).

<sup>&</sup>lt;sup>11</sup> N. D. Mermin and H. Wagner, Phys. Rev. Lett. **17**, 1133 (1966).

<sup>&</sup>lt;sup>12</sup> R. B. Laughlin, private communication (2003).

<sup>&</sup>lt;sup>13</sup> F. J. Wegner, Ann. Physik **3**, 77 (1994).

<sup>&</sup>lt;sup>14</sup> S. D. Głazek and K. G. Wilson, Phys. Rev. D 48, 5863 (1993).

<sup>&</sup>lt;sup>15</sup> S. D. Głazek and K. G. Wilson, Phys. Rev. D **49**, 4214 (1994).

<sup>&</sup>lt;sup>16</sup> S. K. Kehrein and A. Mielke, J. Phys. A: Math. Gen. 27, 4259 (1994).

<sup>&</sup>lt;sup>17</sup> C. Knetter and G. S. Uhrig, Eur. Phys. J. B **13**, 209 (2000).

<sup>&</sup>lt;sup>18</sup> C. P. Heidbrink and G. S. Uhrig, Phys. Rev. Lett. 88, 146401 (2002).

<sup>&</sup>lt;sup>19</sup> C. P. Heidbrink and G. S. Uhrig, Eur. Phys. J. B **30**, 443 (2002).

<sup>&</sup>lt;sup>20</sup> S. R. White, J. Chem. Phys. **117**, 7472 (2002).

<sup>&</sup>lt;sup>21</sup> The Hamiltonian (1) changes the number of DOs only by a single absolute value, namely 2. So the only difference between the matrix elements  $\operatorname{sign}(d_i - d_j)H_{ij}$  and  $(d_i - d_j)H_{ij}$  in an eigen basis of  $\hat{D}$  is a factor of 2.

<sup>&</sup>lt;sup>22</sup> A. Mielke, Eur. Phys. J. B **5**, 605 (1998).

We use the expression "normal-ordering" while we are aware that we are not dealing with conventional normalordering since the strong-coupling problem at hand does not have non-interacting fermions or bosons. Normal-

ordering in the context of the present work refers to the standardized procedure to represent operators.

<sup>&</sup>lt;sup>24</sup> Takahashi gives the 4th order result in Ref. 3. The calculation of the 6th order was done using the method described by Takahashi<sup>3</sup>.

D. G. Pettifor and D. L. Weaire, The Recursion Method and its Applications, Vol. 58 of Springer Series in Solid State Sciences (Springer Verlag, Berlin, 1985).

V. S. Viswanath and G. Müller, The Recursion Method; Application to Many-Body Dynamics, Vol. m23 of Lecture Notes in Physics (Springer-Verlag, Berlin, 1994).

<sup>&</sup>lt;sup>27</sup> P. Fulde, Electron Correlations in Molecules and Solids, Vol. 100 of Solid State Sciences (Springer-Verlag, Berlin, 1993).

<sup>&</sup>lt;sup>28</sup> R. Coldea S. M. Hayden, G. Aeppli, T. G. Perring, C. D. Frost, T. E. Mason, S.-W. Cheong, and Z. Fisk, Phys. Rev. Lett. 86, 5377 (2001).

<sup>&</sup>lt;sup>29</sup> H. J. Schmidt and Y. Kuramoto, Physica **B163**, 443 (1990).

<sup>&</sup>lt;sup>30</sup> Y. Mizuno, T. Tohyama, and S. Maekawa, J. Low Temp. Phys. **117**, 389 (1999).

<sup>&</sup>lt;sup>31</sup> E. Müller-Hartmann and A. Reischl, Eur. Phys. J. B 28, 173 (2002).

<sup>&</sup>lt;sup>32</sup> A. A. Katanin and A. P. Kampf, Phys. Rev. B **66**, 100403 (2002).

<sup>&</sup>lt;sup>33</sup> E. Dagotto, Rev. Mod. Phys. **66**, 763 (1994).

<sup>&</sup>lt;sup>34</sup> S. Nishimoto, F. Gebhard, and E. Jeckelmann, J. Phys.: Condens. Matter 16, 7063 (2004).

<sup>&</sup>lt;sup>35</sup> E. Müller-Hartmann, in *Proceedings of the V. Symposium "Physics of Metals"*, edited by E. Talik and J. Szade (Symposium "Physics of Metals", Ustron-Jaszowiec, Poland, 1991), p. 22.

<sup>&</sup>lt;sup>36</sup> G. S. Uhrig, Phys. Rev. Lett. **77**, 3629 (1996).

<sup>&</sup>lt;sup>37</sup> E. Müller-Hartmann, Z. Phys. B **74**, 507 (1989).

<sup>&</sup>lt;sup>38</sup> R. Bulla, T. A. Costi, and D. Vollhardt, Phys. Rev. B **64**, 045103 (2001).

<sup>&</sup>lt;sup>39</sup> D. J. Garcia, K. Hallberg, and M. J. Rozenberg, cond-mat/0403169.

<sup>&</sup>lt;sup>40</sup> N. Blümer and E. Kalinowski, cond-mat/0404568.